Nafta-Gaz 2025, no. 3, pp. 188–198, DOI: 10.18668/NG.2025.03.05

New calculation method for the pontoon element of offshore fixed platforms for oil and gas production

Nowa metoda obliczeniowa dla elementu pontonowego morskich platform stałych do wydobycia ropy i gazu

Latif F. Aslanov[1,2], Ulvi L. Aslanli[1,2], Firidun L. Aslanov[2]

[1] *"Oil Gas Scientific Research Project" Institute, SOCAR, Azerbaijan*
[2] *Azerbaijan University of Architecture and Construction*

ABSTRACT: Currently, a significant attention is given to the development of fuel and energy resources on the shelf, particularly the oil and gas fields of the Caspian Sea. Addressing this problem requires investigating a broad range of scientific and technical issues. One of the most important problems is the transportation of the support block of offshore platforms, which serves as the main element of hydraulic structures designed for oil and gas production at great depths. This research relates to offshore hydraulic engineering, specifically the construction of offshore platforms whose support structures consist of support blocks transported afloat. The article proposes a method for analyzing and optimizing geometric shapes while considering the physical properties of pontoon materials, enabling the resolution of specific practical problems. The study examines the influence of various factors on the distribution of deformations and stresses in pontoons. A general method for linearizing thin-walled structures with variable geometric parameters is introduced, offering improved convergence. An efficient calculation technique based on the small parameter method is developed. Using these methods, a computational algorithm is formulated, and a set of application programs is established. Accordingly, problems in the general theory of shells are addressed. In structures designed to ensure sufficient strength and manufacturability, all real material properties are considered, leading to more accurate calculation procedures. For a broad class of nonlinear problems in structural mechanics, accounting for the physical properties of materials allows for the identification of additional strength reserves.

Key words: pontoon, support block, offshore platform, shells of rotation, nonlinear model.

STRESZCZENIE: Obecnie wiele uwagi poświęca się rozwojowi zasobów paliw i energii na szelfie, w szczególności złożom ropy naftowej i gazu ziemnego na Morzu Kaspijskim. Rozwiązanie tego problemu wymaga analizy szerokiego zakresu zagadnień naukowych i technicznych. Jednym z kluczowych problemów jest transport bloku podporowego platform morskich, który stanowi główny element konstrukcji hydrotechnicznych przeznaczonych do wydobycia ropy i gazu na dużych głębokościach. Niniejsze badanie dotyczy morskiej inżynierii hydrotechnicznej, a w szczególności budowy platform morskich, których konstrukcje nośne składają się z bloków podporowych transportowanych na wodzie. W artykule zaproponowano metodę analizy i optymalizacji kształtów geometrycznych z uwzględnieniem właściwości fizycznych materiałów, z których wykonane są pontony, umożliwiającą rozwiązanie konkretnych problemów praktycznych. W pracy zbadano wpływ różnych czynników na rozkład odkształceń i naprężeń w pontonach. Przedstawiono ogólną metodę linearyzacji konstrukcji cienkościennych o zmiennych parametrach geometrycznych, oferującą lepszą zbieżność. Opracowano skuteczną technikę obliczeniową opartą na metodzie małego parametru. Korzystając z tych metod, sformułowano algorytm obliczeniowy oraz opracowano zestaw programów użytkowych. W rezultacie rozwiązano problemy z zakresu ogólnej teorii powłok. W konstrukcjach zaprojektowanych w celu zapewnienia wystarczającej wytrzymałości i możliwości produkcji, uwzględniane są wszystkie rzeczywiste właściwości materiałowe, co prowadzi do dokładniejszych procedur obliczeniowych. Dla szerokiej klasy nieliniowych problemów mechaniki konstrukcji, uwzględnienie właściwości fizycznych materiałów pozwala na identyfikację dodatkowych rezerw wytrzymałościowych.

Słowa kluczowe: ponton, blok podporowy, platforma morska, powłoki obrotowe, model nieliniowy.

Corresponding author: L.F. Aslanov, e-mail: *latif.aslanov@bk.ru*

Article contributed to the Editor: 16.08.2024. Approved for publication: 14.03.2025.

Introduction

The support block (SB) is assembled on the slipway of the Baku Deepwater Jackets Plant, named after H. Aliyev. The slipway consists of two parallel slipway beams. The launching track structure includes a concrete base in the coastal section, with a metal deck affixed to it, the upper surface of which forms a sliding plane. To reduce friction during SB movement, a Teflon coating is applied to the sliding paths, ensuring acceptable friction coefficients.

The support block is moved using a push-pull device, which is connected to the support block through a pusher extension by means of connecting units. The weight of the support block is supported by the slipway beams and the rotating frame, with wooden runners installed on the legs of the middle panels of the support block. The force exerted by the push-pull device during support block movement is calculated. To transport the support block along the launching tracks and lower it into the water, launch winches installed on standard concrete foundations are used. Two side winches facilitate the movement of the support block, while the middle winch is employed both for moving the support block and as a braking mechanism. Due to the insufficient displacement of the SB, additional pontoons are installed for launching and transportation. Head pontoons are attached to the side panels of the SB at the front section, while auxiliary pontoons are affixed to the lower panel. The dimensions and placement of the pontoons are determined through calculation.

The permissible value of the distributed linear load on the launching track is dictated by the design of the block, the launching mechanism, and the launching tracks. The maximum distributed linear load is determined based on both the redistribution of loads between the stern and bow skids and the variation of loads along the bow skid length. The distributed linear load on the launching track excreted by the skid with the rotating device is determined. Load calculations involve determining the longitudinal and transverse bending moments acting on the block due to weight and buoyancy forces. These calculations are performed under calm water conditions during transport at a designated draft. Additional loads on submerged SB elements during towing, as well as wave and current impacts, are determined based on the towing speed and the maximum expected wave and current conditions in the transportation area. The stresses from these loads are summed with those arising from the total bending of the block in calm water conditions.

The article of Abdrakhmanova et al. (2023) focuses on the calculation of normal crack openings in a reinforced concrete beam. Agapov et al. (2010) developed three- and quadrangular finite elements of variable thickness, designed for both linear and nonlinear calculations. The stress-deformation state of marine hydrotechnical installations under various loads and effects has been investigated in multiple studies (Aslanov, 2022; Hasanov, 2022; Aslanov and Aslanli, 2024a, 2024b, 2024c; Aslanov and Aslanov, 2024a, 2024b). Avcu et al. (2024) studied dispersion from cracks in the walls of pressure tanks for hydrogen-powered vehicles using a finite element analysis model. Aydin et al. (2020) tested ten samples of thin-walled cylindrical shells in two groups with different dent depths. The test results were compared with various theories and codes. Ayhan (2011) presented a three-dimensional fracture analysis using tetrahedral enhanced elements and a fully unstructured mesh. Bathe et al. (2011) described the application of a 9-node shell element for plate bending problems. Becker (2022) investigated a filled grain silo, estimating allowable yield stress using four different design criteria. The proposed scheme was implemented in the Mathematica program (Borwein and Skerritt, 2012), and the roots of the equations were determined using the secant method (Chapra and Canale, 2014). Bovo et al. (2020) assessed the main characteristics of the dynamic response of vessels and provided lognormal cumulative fragility functions for three different limit states of each vessel. For each limit state, the median and variance parameters of the best-fitting lognormal function of each tank were statistically determined through nonlinear regression analysis. The complete system of equations for shells is typically derived from the equations presented in the three-dimensional theory of elasticity, with additional simplifying assumptions leading to the various shell theories, as discussed by Chapelle and Bathe (2011). Cheng et al. (2022) examined seismic reactions in liquid-solid interactions within a rectangular steel water treatment structure, incorporating different partition opening arrangements using the finite element method. Amaechi et al. (2022) provides a comprehensive review of various offshore petroleum structures, covering the fundamentals of all types of offshore structures (fixed and floating) and the application of these concepts to oil exploration and production. The study presents various design parameters for modern offshore platforms and industry advancements. Chikhi and Djermane (2018) employed a numerical model to evaluate the influence of local geometric imperfections on the dynamic buckling of liquid-filled tanks, modelling the liquid with specific finite elements. Elgridly et al. (2022) conducted three-dimensional modeling using software of V.V. Eliseev and Y.M. Vetyukov (Eliseev and Vetyukov, 2010, 2014) developed on the basis of both Lagrange mechanics and the principle of virtual work. Various applications of this theory are described in several studies (Eliseev et al., 2011; Yeliseyev and Zinovieva, 2014; Filippenko, 2016). Gadjiyev et al. (2023) and Hajiyev et al. (2024) developed an effective numerical method for analyzing

the stress-strain state and load-bearing capacity of compressed concrete pipe elements. When developing the calculation algorithm for compressed concrete, the stress-strain relationship was adopted as a fractional rational function proposed by the Eurocode, while a two-line diagram was adopted for reinforcement.

Gao et al. (2024) report on an ultrashort-channel organic neuromorphic vertical transistor with distributed reservoir states and propose a strategy for developing high-performance reservoir computing networks. Giampieri and Perego (2011) utilize an interface finite element to simulate localized membrane-flexural deformations in shells. An experimental study on the effect of the presence of a pontoon on the movement of a semi-submersible platform with four square columns under flow conditions is presented by Gonçalves et al. (2019). To perform three-dimensional calculations of the stress-strain state, Gontarovskyi et al. (2023) use software based on the finite element method. Gurkalo et al. (2024) conduct a comparative nonlinear dynamic analysis of three-dimensional models for elevated water tanks with different shaft diameters and heights, comparing results of elevated water tanks with slotted and solid reinforced concrete bodies. Hansen and Silva (2022) study the nonlinear oscillations of an elastic-linear multilayer circular cylindrical tank, partially filled with liquid, and with simple support, assuming the reservoir materials to be elastic, linear, and isotropic. Holtschoppen and Knoedel (2024) propose a procedure for reducing overall stresses through a more refined definition of the reservoir reaction, based on the calculation of hydrodynamic pressure and load components dependent on the geometric characteristics of the reservoir. Ibrahimov et al. (2024) present the results of laboratory, experimental, and theoretical research on the development and application of technology ensuring the quality and safety of cementing works to support the filter zone of production wells. T.R Ischanov (2018) develops algorithms for finite element analysis of the stress-strain state of shells, considering transverse shear deformation. Iskandarov (2022) addresses problems related to temperature measurement in thermal energy accounting, proposing solutions to minimize errors by accounting for energy consumption. Ismayilov et al. (2024) describe the design and operating principle of a new expansion device developed to solve the problems associated with the efficient expansion of round steel casing and to achieve double expansion in the construction of wells with a single diameter. In a number of papers (Suleimanov et al., 2008a, 2008b, 2009; 2012, 2018; Suleimanov and Dyshin, 2013; Khabibullin et al., 2022; Jamalbayov et al., 2024), a methodology for hybrid modeling of the development of complex hydrocarbon mixture deposits was developed, comparing the technical and operational performance of pump units based on different kinematic schemes. Khabibullin et al. (2023) propose a method for calculating cylindrical shells in the region of support devices, assuming the shell material to be ideally rigid-plastic.

Khalil et al. (2023) assess the seismic fragility of above-ground steel cylindrical silos intended for storing solid materials. Khosravi and Goudarzi (2023) investigate the seismic risk of cylindrical concrete tanks located on the ground. Kiliç (2021) examines cylindrical water reservoirs under the influence of hydrostatic force or internal vacuum. Kiselev (2013) develops three-dimensional finite elements of various configurations with nodal unknowns in the form of displacements. Kiyamov (2010) describes an efficient method for calculating three-dimensional structural elements with complex curved edges. Kolenchukov et al. (2023) present a review and generalization of data on the parameters and characteristics of rough surfaces. The correlation method, based in the standard deviation of the slope of the roughness profile, is analyzed alongside the effect of secondary flow on coolant behavior in a closed space. Kovtun et al. (2023) conduct theoretical and experimental studies to determine the stresses in elastic-soft tanks during free dropping from an aircraft, aiming to optimize the tank shape and construction. Kumar et al. (2024) investigate the dynamic behavior of a group of piles under different loading directions is studied in a combined case, conducting machine-induced field excitation tests on small-scale hollow steel piles. Labiodh and Chalane (2023) analyze the effect of different positions of localized axisymmetric initial defects on the critical load of elastic cylindrical shells subjected to axial compression, using numerical analysis to evaluate bending resistance. Lebedev et al. (2021) describe the stress-strain state of vertical steel tanks and propose a method for calculating their strength using CAD, considering factors such as uneven foundation settlement, tank wall displacement, and the influence of ring plate dimensions.

Li et al. (2023) discuss the importance of nonlinear terms in the governing equations for describing the short-term large deformation of a thin-walled cylindrical shell under shock pressure. Shubovich (2012) determines the stress-strain state of shells of revolution using both linear and geometrically nonlinear formulations. Mahmood et al. (2022) present a quantitative analysis of eight commonly used methods to identify the most appropriate and reliable interpretation method cast-in-situ piles. Mirsepahi et al. (2021) conduct 3D modeling as part of their study. Majumder and Chakraborty (2021) perform a three-dimensional numerical analysis to examine the response of an underexpanded pile in clay under lateral loading. Jassim et al. (2022) carry out a comprehensive study on optimizing the dimensions of a truncated cone vessel device. Pandian et al. (2024) investigate the determination of the reaction reduction factor applicable to overhead water tanks operating beyond the elastic limit in the earthquake-resistant design.

Raikar and Kangda (2024) explore the application of passive control techniques using a fluid viscous damper to mitigate vibrations and reduce potential damage to water tank structures. Sabaghzadeh and Shafaee (2021) present a numerical method for analyzing the deformation of diaphragm tanks, verified through experimental methods. Santos and Donadon (2023) propose a semi-analytical model using the Ritz method to estimate the axial buckling load and internal pressure behavior of composite cylindrical shells. Sharma et al. (2010) provide an introduction to semisubmersibles along with a critical analysis. Sholomitskii et al. (2023) propose a methodology for converting unstructured laser scan point clouds into a topological equivalent network model, enabling numerical calculation methods for estimating the stress-strain state due to reservoir wall deformations. Sugiura et al. (2024) perform a comparative nonlinear dynamic analysis of three-dimensional models of elevated water tanks with varying shaft diameters and heights using SAP2000 software, comparing results for elevated water tanks with slotted and solid reinforced concrete shafts. Sun et al. (2023) establish a numerical analysis model of liquid-solid coupling to examine the dynamic response and damage of a small domed ACLNG storage tank under penetrating and blast loads. Veliyev et al. (2022) discuss artificial intelligence and its applications in the oil and gas industry, demonstrating how AI can facilitate coordination and cooperation to extend the life cycle of an oil field, improve decision-making, reduce costs, and increase economic efficiency. Wan et al. (2024) analyze the development trend of Compressed Air Energy Storage (CAES) technology and propose a future development path to provide a reference for the study of CAES projects in depleted oil and gas fields. Wang et al. (2011) describe geometrical elements and corrections in the finite element model for the displacement field . Xue et al. (2023) conduct a new theoretical analysis and develop finite element models to investigate the initial residual stress distribution and processing deformation law in a typical aluminum alloy rolled ring. Yang et al. (2024) carry out the first analytical study of the influence of axial variable modulus of elasticity on the bending of thin-walled cylinders subjected to lateral pressure. Yaropolov and Yaropolov (2012) employ rectangular and triangular plane finite elements to solve plane problems of the theory of elasticity . Zhang et al. (2023) conduct an elastoplastic analysis using the finite element method to evaluate the stability of a full-scale reinforced conical steel water tank, incorporating initial defect data obtained from high-resolution laser scanning. In a series of studies by T.V. Zinovieva (2012, 2017), an implicit symmetric one-step difference scheme of second-order accuracy is used for approximating the system equation.

Figure 1 shows a support block positioned on a slipway. The support block is constructed on a slipway that features horizontal launching paths. At the ends of these paths, facing the sea, there are rotating frames adjacent to the slipway cordon. The support block is equipped with runners that rest on the launch paths. The rotating frame contains a rotating component with an upwardly curved cylindrical surface and a foundation with a concentric surface. The launching process is executed as follows.

Under the influence of the pusher force, the support block moves along the launch paths toward the sea. The runners remain in a horizontal position until the center of mass of the support block aligns with the vertical axis of rotation. The pusher continues to propel the support block until its center of mass shifts beyond the vertical axis of rotation, causing the support block together and the swivel frame to tilt. This tilting continues until a portion of the sealed element enters the water at an angle smaller than the friction angle, i.e. $\mathrm{tg}\alpha < f$, where f is the coefficient of friction between the runner and the sliding surface of the rotating frame. The pusher continues to act on the support block until it is fully launched into the water. The rotating frame, featuring an upwardly curved cylindrical surface, is movably articulated with the concentric surface of the foundation. This configuration ensures an even distribution of the load between the rotating frame and the foundation, thereby significantly reducing the metal consumption of the structure.

The technical and economic efficiency of the proposed method and device lies in enabling launches at a water depth of no more than 10 m. This eliminates the need for extensive dredging operations, facilitates the construction of support blocks on horizontal slipways, and allows for their transportation afloat and subsequent launch from the construction slipway into the water. Additionally, this approach enables the construction of support blocks on the same slipways, which can be transferred onto transport and launch barges. These barges receive the support blocks via horizontal launch paths.

A method for sliding a support block onto paired transport pontoons is also considered. In this method, the support block, positioned on lower and head skids, is moved along the launching tracks beyond the assembly site of the cordon onto moored transport pontoons, followed by their subsequent deballasting. To simplify operations and improve reliability, the support block on the lower and head skids is initially slid onto the lower pontoon. During this process, deballasting of the lower pontoon raises the lower end of the support block, allowing for the removal of the lower skids. The support block, now positioned on the lower pontoon and head skids, is further moved until it nears the cordon. The head pontoon is then positioned beneath the upper end of the support block and subsequently deballasted. A device for sliding a support block onto paired transport pontoons, comprising launch paths, lower and head skids and pontoons, is characterized in that each head skid is

made of two parts movably connected along a cylindrical surface. The sliding method follows the sequence described below.

The support block is loaded onto the lower and head skids and moved along the launch paths until it extends beyond the cordon, hanging over the lower pontoon. The head pontoon remains moored nearby and is not involved in the initial sliding operations. Then the lower pontoon is deballasted, lifting the bottom of the support block and causing it to pivot along the cylindrical surface of the head skid. The lower skids are then removed. Next, the support block continues to move along the lower pontoon and head skids until it nears the cordon. The head pontoon is positioned beneath the support block and deballasted. Upon completion of the head pontoon deballasting, the support block separates from the head skid, marking the completion of the sliding process.

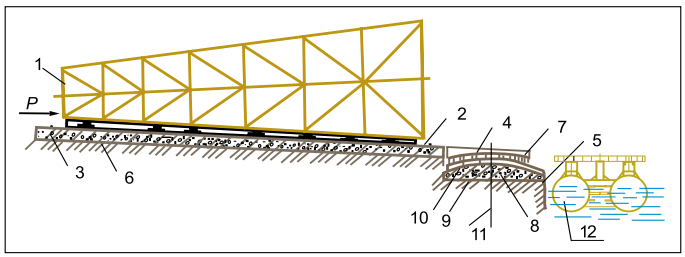

Figure 1. Calculation scheme for lowering the support block into the sea by means of a rotating frame: 1 – support block; 2 – slipway; 3 – horizontal descent paths; 4 – swivel frame; 5 – slipway cordon; 6 – skids; 7 – cylindrical surface; 8 – foundation; 9 – concentric surface; 10 – roller; 11 – vertical axis of rotation; 12 – pontoons

Rysunek 1. Schemat obliczeniowy opuszczania bloku podporowego do morza za pomocą ramy obrotowej: 1 – blok podporowy; 2 – pochylnia; 3 – poziome ścieżki zejścia; 4 – rama obrotowa; 5 – kordon pochylni; 6 – płozy; 7 – powierzchnia cylindryczna; 8 – fundament; 9 – powierzchnia koncentryczna; 10 – rolka; 11 – pionowa oś obrotu; 12 – pontony

Let us determine the stresses and displacements of points on the middle surface of a pontoon, which has the shape of a hemisphere. The pontoon is suspended by its upper edge and filled with a liquid of specific gravity γ N/sm^3 (Figure 2).

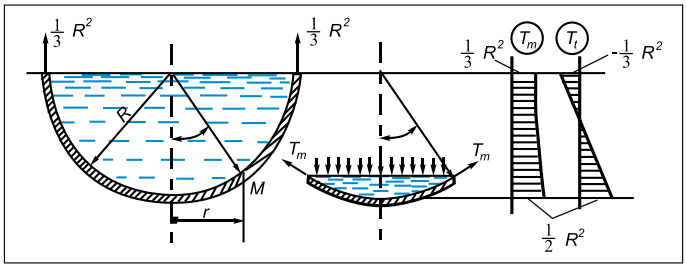

Figure 2. Calculation scheme of the section of the pontoon element

Rysunek 2. Schemat obliczeniowy przekroju elementu pontononowego

Let us consider a section of the pontoon cut off along a circular plane passing through an arbitrary point M. The cut off part is subject to the weight of the liquid in the volume of the segment.

$\gamma V = \gamma\pi R^3(2/3 - \cos\theta + 1/3\cos^2\theta)$ as well as the pressure force from the overlying layers of liquid $p\pi r^2 = \gamma R^3\pi \cos\theta \sin^2\theta$, here $p = \gamma R\cos\theta$ – liquid pressure; $r = R\sin\theta$ – radius of the section circle; γ – specific gravity of liquid. Summing these two forces and dividing by 2π, we obtain the function $F(\theta) = (\gamma R^3)/3\ (1 - \cos^3\theta)$.

Next, using formulas (1) and (2), we determine the forces:

$$T_m = \frac{F(\theta)}{R_t \sin^2\theta} = \frac{\gamma R^2(1-\cos^3\theta)}{3\sin^2\theta} \quad (1)$$

$$T_t = pR_t - T_m\frac{R_t}{R_m} = \gamma R^2\left(\cos\theta - \frac{1-\cos^3\theta}{3\sin^2\theta}\right) \quad (2)$$

In equations (1)–(2), *Tm* and *Tt* – meridional and annular normal forces, respectively; r and θ – coordinates of an arbitrary point; P and R – geometric parameters; γ – weight of the liquid inside the shell. The diagrams of T_m and T_t are shown in Figure 1.

To ensure a momentless state, the upper edge of the hemisphere must be free to move in the radial direction. Let us calculate the changes in both the radius of the upper edge circle and the height of the hemisphere. Let us first determine the relative elongations in the meridional and circumferential directions at an arbitrary point. According to the formulas of the generalized Hooke's law:

$$\varepsilon_m = \frac{T_m - \mu T_t}{Eh} = \frac{\gamma R^2}{3Eh}\left[\frac{1-\cos^3\theta}{\sin^2\theta}(1+\mu) - 3\mu\cos\theta\right] \quad (3)$$

$$\varepsilon_t = \frac{T_t - \mu T_m}{Eh} = \frac{\gamma R^2}{3Eh}\left[3\cos\theta - \frac{1-\cos^3\theta}{\sin^2\theta}(1+\mu)\right] \quad (4)$$

Relative elongation in the circumferential direction of a ring fiber passing through point M:

$$\varepsilon_t = \frac{\xi}{r} = \frac{\xi}{R_t\sin\theta} \quad (5)$$

Radial movement:

$$\xi = \varepsilon_t R_t \sin\theta \quad (6)$$

Meridional deformation:

$$\varepsilon_m = \frac{d\xi}{ds}\cos\theta - \frac{d\eta}{ds}\sin\theta \quad (7)$$

Substituting the value of ε_t into equation (5), we find the radial displacement at an arbitrary point

$$\xi = \varepsilon_t R\sin\theta = \frac{\gamma R^3}{3Eh}\left[\frac{3}{2}\sin 2\theta - \frac{1-\cos^3\theta}{3\sin^2\theta}(1+\mu)\right] \quad (8)$$

Changing the radius of the top edge circle

$$\xi_{\theta=90^\circ} = -\frac{\gamma R^3(1+\mu)}{3Eh} = -0.43\frac{\gamma R^3}{Eh}.$$

$$\eta = \int_{\theta_0}^{\theta}\left(\frac{\varepsilon_m}{\sin\theta} - \frac{d\xi}{R_m d\theta}ctg\theta\right)R_m d\theta \qquad (9)$$

To determine the axial displacement, we use dependence (9) and differentiate ξ by θ:

$$\frac{d\xi}{d\theta} = \frac{\gamma R^3}{3Eh}\left[3\cos 2\theta - 3\cos^2\theta(1+\mu) - \frac{(1-\cos^3\theta)(1+\mu)\cos\theta}{\sin^2\theta}\right] \qquad (10)$$

and substitute $d\xi/d\theta$ and ε_m under the sign (9). After simple transformations, the integral takes the form

$$\eta = \int_0^{90^\circ}\frac{\gamma R^3}{3Eh}\left[(1+\mu)\,\mathrm{tg}\frac{\breve{\theta}}{2} + (2-\mu)\sin 2\breve{\theta}\right]d\breve{\theta}, \quad \text{here } \theta \le \breve{\theta} \le \frac{\pi}{2} \qquad (11)$$

After integrating and substituting $\mu = 0.3$, we obtain the following expression for the axial displacement of an arbitrary point relative to the upper edge:

$$\eta = \left(2.6 + 2.6\ln\cos\frac{\theta}{2} - 1.7\sin^2\theta\right)\frac{\gamma R^3}{3Eh} \qquad (12)$$

For $\theta = 0$, this expression gives the change in the height of the hemisphere, $\eta_{\max} = 2.6(\gamma R^3)/3Eh = 0.86(\gamma R^3)/Eh$.

The plus sign indicates that the height of the hemisphere is increasing. If we take the non-linear deformation as:

$E\varepsilon_m - \beta\varepsilon_m^3$, $E\varepsilon_t - \beta\varepsilon_t^3$ enter $\varepsilon_m = \bar{\varepsilon}_m\varepsilon_0$, $\varepsilon_t = \bar{\varepsilon}_t\varepsilon_0$ and consider that $\nu = \beta\varepsilon_0^2/E \ll 1$ (Aslanov and Aslanli, 2024c).

$$E\varepsilon_m - \beta\varepsilon_m^3 = E\varepsilon_0(\bar{\varepsilon}_m - \nu\bar{\varepsilon}_m^3) \qquad (13)$$

$$E\varepsilon_t - \beta\varepsilon_t^3 = E\varepsilon_0(\bar{\varepsilon}_t - \nu\bar{\varepsilon}_t^3) \qquad (14)$$

Considering (3) and (4) in (13) and (14), respectively:

$$\frac{T_m - \mu T_t}{Eh\varepsilon_0} = \bar{\varepsilon}_0 - \nu\bar{\varepsilon}_m^3 \qquad (15)$$

$$\frac{T_t - \mu T_m}{Eh\varepsilon_0} = \bar{\varepsilon}_t - \nu\bar{\varepsilon}_t^3 \qquad (16)$$

If we write $\bar{\varepsilon}_m$ and $\bar{\varepsilon}_t$ included in (15) and (16) as follows:

$$\bar{\varepsilon}_m = \bar{\varepsilon}_{m_0} + \nu\bar{\varepsilon}_{m_1} + \nu^2\bar{\varepsilon}_{m_2} + \ldots \qquad (17)$$

$$\bar{\varepsilon}_t = \bar{\varepsilon}_{t_0} + \nu\bar{\varepsilon}_{t_1} + \nu^2\bar{\varepsilon}_{t_2} + \ldots \qquad (18)$$

Considering (17), (18) in (15) and (16), respectively:

$$\frac{T_m - \mu T_t}{Eh\varepsilon_0} = \bar{\varepsilon}_{m_0} + \nu(\bar{\varepsilon}_{m_1} - \bar{\varepsilon}_{m_0}^3) + \nu^2(\bar{\varepsilon}_{m_2} - 3\bar{\varepsilon}_{m_0}^5) \qquad (19)$$

$$\frac{T_t - \mu T_m}{Eh\varepsilon_0} = \bar{\varepsilon}_{t_0} + \nu(\bar{\varepsilon}_{t_1} - \bar{\varepsilon}_{t_0}^3) + \nu^2(\bar{\varepsilon}_{t_2} - 3\bar{\varepsilon}_{t_0}^5) \qquad (20)$$

$$\bar{\varepsilon}_{m_0} = \frac{T_m - \mu T_t}{Eh\varepsilon_0};\ \bar{\varepsilon}_{m_1} = \left(\frac{T_m - \mu T_t}{Eh\varepsilon_0}\right)^3;\ \bar{\varepsilon}_{m_2} = 3\left(\frac{T_m - \mu T_t}{Eh\varepsilon_0}\right)^5 \qquad (21)$$

$$\bar{\varepsilon}_{t_0} = \frac{T_t - \mu T_m}{Eh\varepsilon_0};\ \bar{\varepsilon}_{t_1} = \left(\frac{T_t - \mu T_m}{Eh\varepsilon_0}\right)^3;\ \bar{\varepsilon}_{t_2} = 3\left(\frac{T_t - \mu T_m}{Eh\varepsilon_0}\right)^5 \qquad (22)$$

Considering system equations (21) and (22), (17) and (18):

$$\bar{\varepsilon}_{t_0} = (1+\mu)\frac{\gamma R^2}{3Eh}\left(-\frac{1}{1+\cos\theta} + c_1\cos\theta\right)$$

$$\bar{\varepsilon}_{t_1} = \frac{1}{\varepsilon_0^2}(1+\mu)^3\left(\frac{\gamma R^2}{3Eh}\right)^3\left(-\frac{1}{(1+\cos\theta)^3} + 3c_1\frac{\cos\theta}{(1+\cos\theta)^2} - 3c_1^2\frac{\cos^2\theta}{1+\cos\theta} + c_1^3\cos^3\theta\right)$$

$$\bar{\varepsilon}_{t_2} = \frac{3}{\varepsilon_0^4}(1+\mu)^5\left(\frac{\gamma R^2}{3Eh}\right)^4\left(-\frac{1}{(1+\cos\theta)^5} + 5c_1\frac{\cos\theta}{(1+\cos\theta)^4} - 10c_1^2\frac{\cos^2\theta}{(1+\cos\theta)^3} + 10c_1^3\frac{\cos^3\theta}{(1+\cos\theta)^2} - 5c_1^4\frac{\cos^4\theta}{1+\cos\theta} + c_1^5\cos^5\theta\right) \qquad (23)$$

Meridional deformation:

$$\bar{\varepsilon}_{m_0} = (1+\mu)\frac{\gamma R^2}{3Eh}\left(-\frac{1}{1+\cos\theta} + c\cos\theta\right)$$

$$\bar{\varepsilon}_{m_1} = \frac{1}{\varepsilon_0^2}(1+\mu)^3\left(\frac{\gamma R^2}{3Eh}\right)^3\left(-\frac{1}{(1+\cos\theta)^3} + 3c\frac{\cos\theta}{(1+\cos\theta)^2} - 3c^2\frac{\cos^2\theta}{1+\cos\theta} + c^3\cos^3\theta\right)$$

$$\bar{\varepsilon}_{m_2} = \frac{3}{\varepsilon_0^4}(1+\mu)^5\left(\frac{\gamma R^2}{3Eh}\right)^4\left(\frac{1}{(1+\cos\theta)^5} + 5c\frac{\cos\theta}{(1+\cos\theta)^4} - 10c^2\frac{\cos^2\theta}{(1+\cos\theta)^3} + 10c^3\frac{\cos^3\theta}{(1+\cos\theta)^2} - 5c^4\frac{\cos^4\theta}{1+\cos\theta} + c^5\cos^5\theta\right) \qquad (24)$$

here: $c = \frac{1-2\mu}{1+\mu}$, $c_1 = \frac{2-\mu}{1+\mu}$.

Horizontal displacement at an arbitrary point of the middle surface:

$$\bar{\xi}_0 = (1+\mu)\left(\frac{\gamma R^2}{3Eh}\right)\left(-\frac{1}{(1+\cos\theta)^2}+c_1\frac{\cos\theta}{1+\cos\theta}\right)$$

$$\bar{\xi}_1 = \frac{1}{\varepsilon_0^2}(1+\mu)^3\left(\frac{\gamma R^2}{3Eh}\right)^3\left(-\frac{1}{(1+\cos\theta)^3}+3c_1\frac{\cos\theta}{(1+\cos\theta)^2}-3c_1^2\frac{\cos^2\theta}{1+\cos\theta}+c_1^3\cos^3\theta\right)$$

$$\bar{\xi}_2 = \frac{3}{\varepsilon_0^4}(1+\mu)^5\left(\frac{\gamma R^2}{3Eh}\right)^4\left(-\frac{1}{(1+\cos\theta)^5}+5c_1\frac{\cos\theta}{(1+\cos\theta)^4}-10c_1^2\frac{\cos^2\theta}{(1+\cos\theta)^3}+10c_1^3\frac{\cos^3\theta}{(1+\cos\theta)^2}-5c_1^4\frac{\cos^4\theta}{1+\cos\theta}+c_1^5\cos^5\theta\right) \quad (25)$$

$$\bar{\xi}_i = \xi_i / R,\ i = 0 \div 2 \quad (26)$$

Vertical displacement at an arbitrary point:

$$\bar{\eta}_0 = (1+\mu)\left(\frac{\gamma R^2}{3Eh}\right)\left(\cos^2\hat{\theta}+\ln(1+\cos\hat{\theta})\right)$$

$$\bar{\eta}_1 = \frac{1}{\varepsilon_0^2}(1+\mu)^3\left(\frac{\gamma R^2}{3Eh}\right)^3\int_{\theta}^{90^\circ}\left(-\frac{1}{\sin^2\theta}\left(\frac{2}{(1+\cos\hat{\theta})^3}+3(c-c_1)\frac{\cos\hat{\theta}}{(1+\cos\hat{\theta})^2}+3(c^2+c_1^2)\frac{\cos\hat{\theta}}{1+\cos\hat{\theta}}\right)\right)d\cos\hat{\theta}$$

$$\eta_2 = \frac{1}{\varepsilon_0^4}(1+\mu)^5\left(\frac{\gamma R^2}{3Eh}\right)^5\int_{\theta}^{90^\circ}\left(-\frac{1}{\sin^2\theta}\left(\frac{2}{(1+\cos\hat{\theta})^5}+5(c-c_1)\frac{\cos\hat{\theta}}{(1+\cos\hat{\theta})^4}+10(c^2+c_1^2)\frac{\cos^2\hat{\theta}}{(1+\cos\hat{\theta})^3}+10(c^3-c_1^3)\frac{\cos^3\hat{\theta}}{(1+\cos\hat{\theta})^2}\right.\right.$$
$$\left.\left.+5(c^4+c_1^4)\frac{\cos^4\hat{\theta}}{1+\cos\hat{\theta}}+(c^5-c_1^5)\cos^5\hat{\theta}\right)\right)d\cos\hat{\theta},\ \theta\le\hat{\theta}\le\frac{\pi}{2} \quad (27)$$

A thin-walled hemispherical shell with variable geometric parameters was studied taking into account physical nonlinearity and boundary conditions. Analytical expressions for displacements, stresses, and meridional and annular forces were derived. In the new modification, the series obtained using the nonlinear elastic body model and the small parameter method are quickly collected, which leads to a significant simplification of the calculations.

Materials and methods

The purpose of the study is to determine the actual stress-deformation state occuring in pontoons used for the launching and installation of the support block of a stationary offshore platform, considering the existing water depth. Given the material properties of the pontoon, the stress variation as a function of deformation is analyzed using a nonlinear model. An integrated approach was adopted, incorporating scientific analysis, planning, and conducting research. The problems posed in the study were solved using methods of mathematical analysis, numerical modeling, basic rules of structural mechanics, mechanics of deformable solids, elasticity theory and finite difference method. Theories of strength and stability were applied to assess the launching, transportation, and installation of the support block of the stationary offshore platform at the construction site. Both analytical and numerical calculation methods were employed, and the results were compared. Block launching simulations were conducted using the "LAUNCH" subprogram of the SACS software.

The objectives of the study are to develop new versions of formulas for specifying the middle surfaces of arbitrary shells, allowing to calculate shells without imposing significant restrictions on their dimensions. Various displacements occurring in the cross-sections of the pontoon structure are considered as a series. By introducing a small parameter into the series, an analytical solution of the displacement change is obtained and the existing calculation methods are improved. A physical nonlinear elastic body model is used to study the stress-strain state, and the reliability of the results obtained is verified by mathematical methods. A nonlinear body model is used to study the stress-strain state. To check the accuracy of the calculation results, the system of obtained equations, considered on a number of numerical examples, was solved by known methods. In this case, some of the results were compared with the works of other authors and it was found that the results coincide.

Results and discussion

The stress-strain state of oil field structures is determined taking into account various loading conditions, and new methods for calculating structures on its basis are developed and applied to solve practical problems. Based on an axially loaded nonlinear model, a cylindrical shell is analyzed while accounting for changes in geometric parameters. The calculation of

a symmetrically loaded coating structure is performed, accounting for the physical properties of the material and changes in geometric parameters. Oil field structures are calculated taking into account internal pressure and a calculation method is developed based on the small parameter method. The coating is analyzed taking into account external and internal impacts, symmetric and asymmetric loads, and stiffeners, with optimal geometric dimensions determined for a wide range of materials. In the first approach, stress decreased by 12.7% compared to the linear model, in the second approach by 8.2%, in the third approach by 5.2%, and in another case by 8.3% due to a change in the geometric parameter. The accuracy and convergence of the constructed numerical scheme are studied using test examples. A comparison was made between the results obtained in the linear and nonlinear formulations (Figure 3).

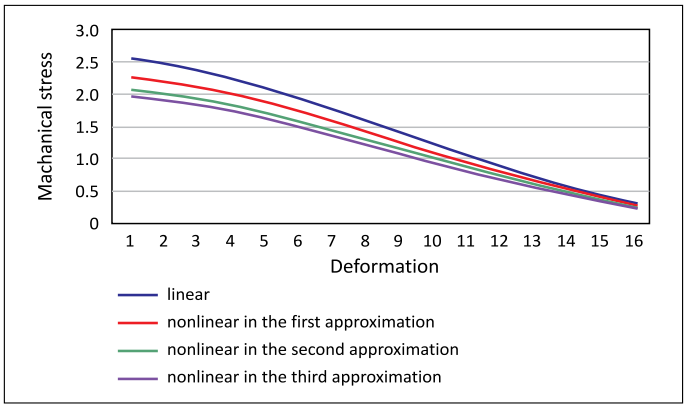

Figure 3. Graph of stress changes in the meridional direction
Rysunek 3. Wykres zmian naprężeń w kierunku południkowym

Conclusion

In this study, the processes of lowering the support block of the stationary offshore platform into the sea through the rotating frame, launching it, and setting it on the seabed at the construction site are analyzed. The results of the study allow for the use of new calculation methods based on nonlinearity in the construction and design of hydraulic structures. The research methodology used in studying the stress-strain state of enclosing structures can be widely applied in the practice of designing such structures and can also serve as a methodological tool for assessing the strength of existing enclosing structures. The proposed calculation methods allow for the accurate determination of the impact of static loads on oil field facilities, improving existing calculation methods and, most importantly, achieving technical efficiency. The use of nonlinear theory enables a more precise stress calculation, allowing for the selection of optimal dimensions and cross-sectional shapes of structural elements. Based on the calculation results, formulas and methods have been compiled that can be used in engineering practice. A solution has been obtained for coatings of circular cross-section, with constant and conical thickness, under external load, as well as internal pressure, taking into account the impact of asymmetric and symmetric loads based on small parameter methods.

A method for calculating the strength of shells of revolution of variable thickness, made of nonlinear elastic material, has been developed, considering surface loads and post-critical deformation. The scope of application of the developed methods for calculating the strength of shells made of nonlinear elastic material, with different methods of specifying boundary conditions, has been established. The accuracy and convergence of the constructed numerical scheme have been studied using test examples. A comparison of the results obtained in linear and nonlinear formulations has been carried out.

References

Abdrakhmanova L.K., Mukhamadiyarov A.V., Suleymanov I.I., Kholkin N.A., Yakovleva A.F., 2023. Calculation of normal crack opening width of reinforced concrete beams under bending. *SOCAR Proceedings*, 1: 131–134. DOI: 10.5510/OGP20230100815.

Agapov V.P., Bardysheva Yu.A., Minakov S.A., 2010. Accounting for physical and geometric nonlinearity in calculations of reinforced concrete slabs and shells of variable thickness by the finite element method. *Structural Mechanics and Analysis of Constructions*, 5: 62–66.

Amaechi C.V., Reda A., Butler H.O., Ja'e I.A., An C., 2022. Review on fixed and floating offshore structures. Part I: types of platforms with some applications. *Journal of Marine Science and Engineering*, 10(8): 1074. DOI: 10.3390/jmse10081074.

Aslanov L.F., 2022. Optimization of the calculation of the piles of fixed offshore platforms. [In:] El-Askary H., Erguler Z.A., Karakus M., Chaminé H.I. (eds.), Research developments in geotechnics, geo-informatics and remote sensing. CAJG 2019. *Advances in Science, Technology & Innovation. Springer, Cham*. DOI: 10.1007/978-3-030-72896-0_32.

Aslanov L.F., Aslanli U.L., 2024a. Determination of load-bearing capacity of piles used in stationary offshore platforms. *SOCAR Proceedings*, 1: 116–123. DOI: 10.5510/OGP20240100949.

Aslanov L.F., Aslanli U.L., 2024b. Study of marine hydraulic structures under seismic effects. [In:] Ksibi M., Sousa A., Hentati O., Chenchouni H. Velho J.L., Negm A., Rodrigo-Comino J., Hadji R., Chakraborty S., Ghorbal A. [eds]. Recent advances in environmental science from the Euro-Mediterranean and surrounding regions. 4th Edition. EMCEI 2022. *Advances in Science, Technology & Innovation. Springer, Cham*. DOI: 10.1007/978-3-031-51904-8_193.

Aslanov L.F., Aslanli U.L., 2024c. Study of the stress-strain state of the pontoon element of the support block. *SOCAR Proceedings*, 2: 115–121. DOI: 10.5510/OGP20240200976.

Aslanov L.F., Aslanov F.L., 2024a. Choosing an effective design solution for fixing offshore hydro-technical structures to shelf ground. [In:] Çiner A., et al. Recent research on geotechnical engineering, remote sensing, geophysics and earthquake seismology. MedGU 2021. *Advances in Science, Technology & Innovation. Springer, Cham*. DOI: 10.1007/978-3-031-43218-7_22.

Aslanov L.F., Aslanov F.L., 2024b. Some tasks of increasing and identifying the reserves of the bearing capacity of anchor fastenings

of offshore fixed platforms. [In:] Bezzeghoud M., et al. Recent research on geotechnical engineering, remote sensing, geophysics and earthquake seismology. MedGU 2022. *Advances in Science, Technology & Innovation. Springer, Cham*. DOI: 10.1007/978-3-031-48715-6_10.

Avcu A., Seyedzavvar M., Boğa C., Choupani N., 2024. Characterizing the effects of liner and fiber-reinforced resin composite shell on fracture energy in type-III high-pressure composite tanks. *Journal of the Brazilian Society of Mechanical Sciences and Engineering*, 46: 13. DOI: 10.1007/s40430-023-04598-9.

Ayhan A.O., 2011. Three-dimensional fracture analysis using tetrahedral enriched elements and fully unstructured mesh. *International Journal of Solids and Structures*, 48(3–4): 492–505. DOI: 10.1016/j.ijsolstr.2010.10.012.

Aydin A.C., Yaman Z., Ağcakoca E., Kiliç M., Maali M., Dizaji A.A., 2020. CFRP Effect on the buckling behavior of dented cylindrical shells. *International Journal of Steel Structures*, 20: 425–435. DOI: 10.1007/s13296-019-00294-4.

Bathe K.-J., Brezzi F., Marini L., 2011. The MITC9 shell element in plate bending: Mathematical analysis of a simplified case. *Computational Mechanics*, 47(6): 617–626. DOI: 10.1007/s00466-010-0565-2.

Becker W.T., 2022. Brittle fracture in a large grain storage bin. *Journal of Failure Analysis and Prevention*, 22: 2012–2022. DOI: 10.1007/s11668-022-01505-7.

Borwein J.M., Skerritt M.B., 2012. An introduction to modern mathematical computing: with mathematica. *Springer New York*. DOI: 10.1007/978-1-4614-4253-0.

Bovo M., Barbaresi A., Torreggiani D., 2020. Definition of seismic performances and fragility curves of unanchored cylindrical steel legged tanks used in wine making and storage. *Bulletin of Earthquake Engineering*, 18: 3711–3745. DOI: 10.1007/s10518-020-00841-z.

Chapelle D., Bathe K.J., 2011. The finite element analysis of shells - fundamentals, computational fluid and solid mechanics. 2nd Edition. *Springer Berlin, Heidelberg*. DOI: 10.1007/978-3-642-16408-8.

Chapra S.C., Canale R.P., 2014. Numerical methods for engineers. *McGraw-Hill Education, New York*.

Cheng X., Chen J., Luo B., 2022. Reduced sloshing effect in steel tanks. *International Journal of Steel Structures*, 22: 1474–1496 DOI: 10.1007/s13296-022-00652-9.

Chikhi A., Djermane M., 2018. Effect of local geometrical imperfection on dynamic buckling of cylindrical storage tanks. *Asian Journal of Civil Engineering*, 19: 189–203. DOI: 10.1007/s42107-018-0017-4.

Elgridly E.A., Fayed A.L., Ali A.A., 2022. Efficiency of pile groups in sand soil under lateral static loads. *Innovative Infrastructure Solutions*, 7: 26. DOI: 10.1007/s41062-021-00628-4.

Eliseev V.V., Vetyukov Y.M., 2010. Finite deformation of thin shells in the context of analytical mechanics of material surfaces. *Acta Mechanica*, 209: 43–57. DOI: 10.1007/s00707-009-0154-7.

Eliseev V.V., Vetyukov Y.M., 2014. Theory of shells as a product of analytical technologies in elastic body mechanics. *Shell Structures: Theory and Applications*, 3: 81–85. DOI: 10.1201/b15684-18.

Eliseev V.V., Vetyukov Y.M., Zinov'eva T.V., 2011. Divergence of a helicoidal shell in a pipe with a flowing fluid. *Journal of Applied Mechanics and Technical Physics*, 52: 450–458. DOI: 10.1134/S0021894411030151.

Filippenko G.V., 2016. The vibrations of reservoirs and cylindrical supports of hydro technical constructions partially submerged into the liquid. [In:] Evgrafov A. (ed). Advances in mechanical engineering, lecture notes in mechanical engineering. *Springer*, Cham. DOI: 10.1007/978-3-319-29579-4_12.

Gadjiyev M.A., Guseynov I.G., Gadjiyeva U.M., 2023. Stress-strain state and load ability of compressed pipe-concrete elements. *SOCAR Procedings*, SI1: 21–26. DOI: 10.5510/OGP2023SI100836.

Gao C., Liu D., Xu C., Xie W., Zhang X., et al., 2024. Toward grouped-reservoir computing: organic neuromorphic vertical transistor with distributed reservoir states for efficient recognition and prediction. *Nature Communications*, 15: 740. DOI: 10.1038/s41467-024-44942-8.

Giampieri A., Perego U., 2011. An interface finite element for the simulation of localized membrane-bending deformation in shells. *Computer Methods in Applied Mechanics and Engineering*, 200(29–32): 2378–2396. DOI: 10.1016/j.cma.2011.04.009.

Gonçalves R.T., Suzuki H., Cenci F., Fujarra A.L.C., Hirabayashi S., 2019. Experimental study of the effect of the pontoon presence on the flow-induced motion of a semi-submersible platform with four square columns. *ASME 2019 38th International Conference on Ocean, Offshore and Arctic Engineering. Vol. 9: Rodney Eatock Taylor Honoring Symposium on Marine and Offshore Hydrodynamics; Takeshi Kinoshita Honoring Symposium on Offshore Technology. Glasgow, Scotland, UK*. DOI: 10.1115/OMAE2019-95250.

Gontarovskyi P.P., Smetankina N.V., Garmash N.G., Melezhyk I.I., Protasova T.V., 2023. Three-dimensional stress-strain state analysis of the bimetallic launch vehicle propellant tank shell. *Strength of Materials*, 55: 916–926. DOI: 10.1007/s11223--023-00582-9.

Gurkalo F., He C., Poutos K., He N., 2024. Effects of innovative reinforced concrete slit shaft configuration on seismic performance of elevated water tanks. *Scientific Reports*, 14: 6113. DOI: 10.1038/s41598-024-56851-3.

Hajiyev M.A., Huseynov I.G., Hajiyeva U.M., Alaeva S.M., 2024. Calculation of metal elements deflection using a three-line strain diagram. *SOCAR Proceedings*, 2: 109–114. DOI: 10.5510/OGP20240200975.

Hansen E.L.M.B., Silva F.M.A., 2022. Nonlinear vibration analysis of a partially filled multi-layer cylindrical tank: consideration of the sloshing effects in the fluid–structure interaction. *Journal of the Brazilian Society of Mechanical Sciences and Engineering*, 44: 484. DOI: 10.1007/s40430-022-03800-8.

Hasanov F.G., 2022. Sress-strain analysis and optimization of the geometric shape of cylindrical oilfield reservoirs. *SOCAR Proceedings*, SI2: 48–52. DOI: 10.5510/OGP2022SI200749.

Holtschoppen B., Knoedel P., 2024. Seismic response of slender storage tanks on tube feet or skirt support. *Bulletin of Earthquake Engineering*, 22: 55–73. DOI: 10.1007/s10518-023-01704-z.

Ibrahimov Kh.M., Hajiyev A.A., Huseynova N.I., Asadova G.Sh., 2024. Consideration of the geological and technical condition of the reservoir and wellbore bottom zone in the selection of the cement composition applied to the production wellbore flow zone. *Scientific Petroleum*, 1: 36–43. DOI: 10.53404/Sci.Petro.20240100055.

Ishanov T.R., 2018. Finite-element analysis of the stress-strain state of thin shells taking into account the transverse shear for various variants of approximation of angular displacements. *PhD Thesis. VSU, Volgograd*.

Iskandarov N.Sh., 2022. Improving the accuracy of temperature measurements in heat supply systems. *SOCAR Proceedings*, 2: 84–87. DOI: 10.5510/OGP20220200679.

Ismayilov Sh.Z., Shmoncheva Y.Y., Jabbarova G.V., 2024. Development of expandable pipe technology: double-acting expander. *Scientific Petroleum*, 1: 44–49. DOI: 10.53404/Sci.Petro.20240100056.

Jamalbayov M.A., Hasanov I.R., Dogan M.O., Jamalbayli T.M., 2024. A hybrid modeling approach: dynamic simulation of two-phase fluid flow in compacting gas condensate reservoirs using potential flow theory. *Scientific Petroleum*, 1: 28–35. DOI: 10.53404/Sci.Petro.20240100054

Jassim A., Ganjian N., Eslami A., 2022. Design and fabrication of frustum confining vessel apparatus for model pile testing in saturated soils. *Innovative Infrastructure Solutions*, 7, 280. DOI: 10.1007/s41062-022-00877-x.

Khabibullin M.Ya., Bakhtizin R.N., Gilaev G.G., 2022. A new method of designing a conversing mechanism of a hinged four-link of a pumping machine. *SOCAR Proceedings*, 2: 93–99. DOI: 10.5510/OGP20220200681.

Khabibullin M.Ya., Gilaev G.G., Bakhtizin R.N., 2023. Improvement of calculated strength indicators of cylindrical shells to reduce the metal consumption of equipment. *SOCAR Proceedings*, 2: 111–117. DOI: 10.5510/OGP20230200853.

Khalil M., Ruggieri S., Tateo V., Nascimbene R., Uva G., 2023. A numerical procedure to estimate seismic fragility of cylindrical ground-supported steel silos containing granular-like material. *Bulletin of Earthquake Engineering*, 21: 5915–5947. DOI: 10.1007/s10518-023-01751-6.

Khosravi S., Goudarzi M.A., 2023. Seismic risk assessment of on-ground concrete cylindrical water tanks. *Innovative Infrastructure Solutions*, 8: 68. DOI: 10.1007/s41062-022-01002-8.

Kiliç M., 2021. Buckling behavior of nose cone type steel tanks including horizontal imperfection. *International Journal of Steel Structures*, 21: 1408–1419. DOI: 10.1007/s13296-021-00512-y.

Kiselev A.P., 2013. Linear and nonlinear deformation of elastic bodies based on three-dimensional FE with variable interpolation of displacements. *PhD Thesis. VSU, Volgograd*.

Kiyamov Kh.G., 2010. Spline version of the finite element method for calculating the conjugation region of shells of complex geometry. [In:] *23rd International Scientific Conference: Mathematical Methods in Technology and Technology, SSTU, Saratov, 28–29 June*.

Kolenchukov O.A., Kolenchukova T.N., Bashmur K.A., Bukhtoyarov V.V., Sergienko R.B., 2023. Discrete rough surface intensifiers in the thermal decomposition plants: current status and future potential. *SOCAR Proceedings*, SI1: 1–8. DOI: 10.5510/OGP2023SI100823.

Kovtun A.V., Tabunenko V.O., Nesterenko S., Ivanchenko O.V., 2023. Determining the strength of tanks with fluid in the case of free dropping. *International Applied Mechanics*, 59: 107–113. DOI: 10.1007/s10778-023-01204-2.

Kumar S., Choudhary S.S., Burman A., 2024. Machine induced dynamic field responses of group pile with different pile arrangements. *Geo-Engineering*, 15: 8. DOI: 10.1186/s40703-024-00207-3.

Labiodh B., Chalane M., 2023. Effect of localized defect positioning on buckling of axisymmetric cylindrical shells under axial compression. *Mechanics of Solids*, 58: 880–889. DOI: 10.3103/S0025654423600046.

Lebedev A.E., Kapranova A.B., Gudanov I.S., Dolgin D.S., Vatagin A.A., 2021. Study of the influence of annular plate size on the stress-strain state of a vertical steel tank. *Chemical and Petroleum Engineering*, 57: 239–245. DOI: 10.1007/s10556-021-00924-x.

Li Y., Fu J., Qian L., Wang H.Y., 2023. On the discussions of nonlinear terms in the large deformation model of thin-walled cylindrical shells. *Mechanics of Solids*, 58: 1214–1227. DOI: 10.3103/S0025654423600216 .

Mahmood A., Alshameri B., Khalid M. H., Muhammad Jamil S., 2022. Comparative study of various interpretative methods of the pile load test. *Innovative Infrastructure Solutions*, 7: 102. DOI: 10.1007/s41062-021-00697-5.

Majumder M., Chakraborty D., 2021. Three-dimensional numerical analysis of under-reamed pile in clay under lateral loading. *Innovative Infrastructure Solutions*, 6: 55. DOI: 10.1007/s41062-020-00428-2.

Mirsepahi M., Nayeri A., Lajevardi S.H., Mirhosseini S.M., 2021. Effect of multi-faced twin tunneling in different depths on a single pile. *Innovative Infrastructure Solutions*, 6, 42. DOI: 10.1007/s41062-020-00425-5.

Pandian A.V.P., Arunachalam K.P., Avudaiappan S., Jasmin S.S., Bendezu Romero L.M., Awoyera P.O., 2024. Modification of response reduction factors of overhead water tanks based on ductility factor. *Discover Applied Sciences*, 6: 192. DOI: 10.1007/s42452-024-05762-z.

Raikar R.G., Kangda M.Z., 2024. Blast mitigation of elevated water tanks equipped with resilient fluid viscous dampers. *Innovative Infrastructure Solutions*, 9: 238. DOI: 10.1007/s41062-024-01536-z.

Sabaghzadeh H., Shafaee M., 2021. Reversal modeling and optimal design of hyper-elastic diaphragm in space fuel tanks. *SN Applied Sciences*, 3: 792. DOI: 10.1007/s42452-021-04785-0.

Santos P.R., Donadon M.V., 2023. A semi-analytical model for buckling and stress analyses of pressurized composite cylinders. *Journal of the Brazilian Society of Mechanical Sciences and Engineering*, 45: 484. DOI: 10.1007/s40430-023-04350-3.

Sharma R., Kim T.-W., Sha O.P., Misra S.C., 2010. Issues in offshore platform research – Part 1: Semi-submersibles. *International Journal of Naval Architecture and Ocean Engineering*, 2(3): 155–170. DOI: 10.3744/JNAOE.2010.2.3.155.

Sholomitskii A.A., Tsarenko S.N., Mogilny S.G., Aukazhieva Z.M., Kemerbaev N.T., 2023. Evaluation of stress-strain state of vertical steel tanks using laser scanning data. [In:] Radionov A.A., Gasiyarov V.R. (eds.), Proceedings of the 8th International Conference on Industrial Engineering. ICIE 2022. *Lecture Notes in Mechanical Engineering. Springer, Cham*. DOI: 10.1007/978-3-031-14125-6_86.

Shubovich A.A., 2012. Analysis of the stress-strain state of shells of revolution in a geometrically nonlinear formulation with different variants of displacement interpolation. *PhD Thesis. VSU, Volgograd*.

Sugiura S., Ariizumi R., Asai T., Azuma S.-I., 2024. Existence of reservoir with finite-dimensional output for universal reservoir computing. *Scientific Reports*, 14: 8448. DOI: 10.1038/s41598-024-56742-7.

Suleimanov B.A., Abbasov E.M., Dyshin O.A., 2008a. Application of wavelet transforms to the solution of boundary value problems for linear parabolic equations. *Computational Mathematics and Mathematical Physics*, 48(2): 251–268. DOI: 10.1134/S0965542508020085.

Suleimanov B.A., Abbasov E.M., Dyshin O.A., 2008b. Wavelet method for solving the unsteady porous-medium flow problem with discontinuous coefficients. *Computational Mathematics and Mathematical Physics*, 48(12): 2194–2210. DOI: 10.1134/S0965542508120099.

Suleimanov B.A., Abbasov E.M., Dyshin O.A., 2009. Wavelet method for solving second-order quasilinear parabolic equations with a conservative principal part. *Computational Mathematics and Mathematical Physics*, 49(9): 1554–1566. DOI: 10.1134/S0965542509090103.

Suleimanov B.A., Dyshin O.A., 2013. Application of discrete wavelet transform to the solution of boundary value problems for quasilinear parabolic equations. *Applied Mathematics and Computation*, 219: 7036–7047. DOI: 10.1016/j.amc.2012.11.033.

Suleimanov B.A., Ismailov F.S., Dyshin O.A., Guseynova N.I., 2012. Analysis of oil deposit exploration state on the base of multifractal approach. *SOCAR Proceedings*, 2: 20–28. DOI: 10.5510/OGP20120200110.

Suleimanov B.A., Ismailov F.S., Huseynova N.I., Veliev E.F., 2018. The application of fuzzy logic and multi-fractal analysis for reservoir management. *Proceedings of The 6th International Conference on Control and Optimization with Industrial Applications*, 1: 34–36.

Sun Y., Wang C., Wang W., Li T., Yang T., 2023. Dynamic response analysis of a small-scaled ACLNG storage tank under penetration and explosion loadings. *Acta Mechanica Sinica*, 39: 123110. DOI: 10.1007/s10409-023-23110-x.

Veliyev E.F., Shirinov S.V., Mammedbeyli T.E., 2022. Intelligent oil and gas field based on artificial intelligence technology. *SOCAR Proceedings*, 4: 70–75. DOI: 10.5510/OGP20220400785.

Wan J., Sun Y., He Y., Ji W., Li J., Jiang L., Jurado M.J., 2024. Development and technology status of energy storage in depleted gas reservoirs. *International Journal of Coal Science & Technology*, 11: 29. DOI: 10.1007/s40789-024-00676-y.

Wang W., Mottershead J.E., Sebastian S.M., Patterson E. A., 2011. Shape features and finite'element model updating from full-field strain date. *International Journal of Solids and Structures*, 48(11–12): 1644–1657. DOI: 10.1016/j.ijsolstr.2011.02.010.

Xue N.P., Wu Q., Yang R.S., Gao H.-J., Zhang Z., Zhang Y.-D., Li L., Guo J., 2023. Research on machining deformation of aluminum alloy rolled ring induced by residual stress. *The International Journal of Advanced Manufacturing Technology*, 125: 5669–5680. DOI: 10.1007/s00170-023-11068-y.

Yang L., Zhang S., Qiu T., 2024. Buckling analyses of cylindrical shells with axial variable elastic modulus under external pressure. *Journal of the Brazilian Society of Mechanical Sciences and Engineering*, 46: 163. DOI: 10.1007/s40430-024-04742-z.

Yaropolov V.A., Yaropolov Yu.V., 2012. Study of the influence of initial deviations of the shape of a spherical shell on stability by the finite element method. *Advances in Current Natural Sciences*, 6: 127–128.

Yeliseyev V.V., Zinovieva T.V., 2014. Two-dimensional (shell-type) and three-dimensional models for elastic thin-walled cylinder. *PNRPU Mechanics Bulletin*, 3: 50–70. DOI: 10.15593/perm.mech/2014.3.04.

Zhang H., Ansary A.M.E., Zhou W., 2023. Nonlinear buckling analysis of conical steel tanks considering field-measured imperfections – a case study. *Proceedings of the Canadian Society of Civil Engineering Annual Conference, CSCE 2021. Springer, Singapore*. DOI: 10.1007/978-981-19-0507-0_28.

Zinovieva T.V., 2012. Computational mechanics of elastic shells of revolution in mechanical engineering calculations. [In:] Zinovieva T.V. (eds.), Modern engineering: science and education. *State Polytechnic University, Saint Petersburg*.

Zinovieva T.V., 2017. Calculation of shells of revolution with arbitrary meridian oscillations. [In:] Evgrafov A. (eds.), Advances in mechanical engineering. Lecture notes in mechanical engineering. *Springer, Cham*. DOI: 10.1007/978-3-319-53363-6_17.

Latif Firudin ASLANOV, Ph.D.
Scientist at the "Oil Gas Scientific Research Project" Institute, SOCAR
88a Zardabi Ave., AZ1122 Baku, Azerbaijan
Associate Professor at the Azerbaijan University of Architecture and Construction
5 Ayna Sultanova St., AZ1073 Baku, Azerbaijan
E-mail: *latif.aslanov@bk.ru*

Ulvi Latif ASLANLI, M.Sc.
Senior structural engineer at the "Oil Gas Scientific Research Project" Institute, SOCAR, Baku, Azerbaijan
Ph.D. Candidate, Lecturer at the Azerbaijan University of Architecture and Construction, Baku, Azerbaijan
E-mail: *ulvi.l.aslanli@socar.az*

Firidun Latif ASLANOV, M.Sc.
Ph.D. Candidate at the Azerbaijan University of Architecture and Construction
5 Ayna Sultanova St., AZ1073 Baku, Azerbaijan
E-mail: *firidun-aslanov@mail.ru*